THE CHRONOLOGY OF TELL EL-DABA: A CRUCIAL MEETING POINT OF ^{14}C DATING, ARCHAEOLOGY, AND EGYPTOLOGY IN THE 2ND MILLENNIUM BC

Walter Kutschera[1,2] • Manfred Bietak[3,4] • Eva Maria Wild[1] • Christopher Bronk Ramsey[5] • Michael Dee[5] • Robin Golser[1] • Karin Kopetzky[3] • Peter Stadler[6,7] • Peter Steier[1] • Ursula Thanheiser[4] • Franz Weninger[1]

ABSTRACT. Radiocarbon dating at the Tell el-Daba site in the Nile Delta has created an enigma for many years. Despite great efforts, the difference of about 120 yr between the chronology based on ^{14}C dates and the one based on archaeological evidence linked to the Egyptian historical chronology has not been solved. In order to foster open discussions on this discrepancy, we present here the results of 40 ^{14}C accelerator mass spectrometry (AMS) measurements on short-lived plant material assigned to 14 different phases of the Tell el-Daba excavation, spanning 600 yr (about 2000–1400 BC). On the one hand, the recently established agreement between ^{14}C dates and dynastic Egypt (Bronk Ramsey et al. 2010) makes it unlikely that the problem lies in the ^{14}C dates and/or the Egyptian historical chronology. On the other hand, the extensive archaeological evidence from Tell el-Daba linked to many different cultures in the eastern Mediterranean and to the Egyptian historical chronology provides strong evidence for an absolute chronology shifted by about 120 yr with respect to the ^{14}C dates.

INTRODUCTION

Before radiocarbon was introduced as a dating tool, the historical chronology of ancient Egypt provided the only absolute timeframe for the Bronze and Iron ages in the eastern Mediterranean. Recently, it has been shown (Bronk Ramsey et al. 2010) that with the application of Bayesian analysis including relative historical data from Egypt, ^{14}C dating and the Egyptian chronology agree well with each other for the dynastic periods in Egypt.

For the 2nd millennium BC, extensive archaeological investigations during the last 30 yr established relative chronologies in many regions of the eastern Mediterranean (Aegean, Anatolia, Levant, Egypt). In order to establish an absolute timeframe for archaeological sites, they depend either on material (e.g. ceramic imports) with direct links to the Egyptian chronology and/or on ^{14}C dating. The overall goal is to find a consensus between these 3 pillars of chronology (archaeology, ^{14}C dating, and Egyptology), thus synchronizing the cultural relations between the different civilizations in a consistent way.

An important time marker in the middle of the 2nd millennium BC is the cataclysmic volcanic eruption of Thera/Santorini, which has been traced by "fingerprinting" of tephra in various regions of the eastern Mediterranean (e.g. Steinhauser et al. 2006, 2010; Bruins et al. 2008; Sterba et al. 2009). Despite numerous efforts to pin down this date through archaeological evidence linked to the Egyptian chronology and by ^{14}C dating, no consensus between both methods has yet been reached (Balter 2006; Friedrich et al. 2006, 2009; Manning et al. 2006, 2009a; Bietak and Höflmayer 2007; Wiener 2009; Bruins 2010; Bietak 2012). In general, ^{14}C dating points to an eruption in the second half of the 17th century BC. This time range seems to be supported by various other—albeit less direct—

[1]University of Vienna, Faculty of Physics, Vienna Environmental Research Accelerator (VERA) Laboratory, Vienna, Austria.
[2]Corresponding author. Email: walter.kutschera@univie.ac.at.
[3]Austrian Academy of Sciences, Commission for Egypt and the Levant, Vienna, Austria.
[4]University of Vienna, Vienna Institute for Archaeological Science (VIAS), Vienna, Austria.
[5]Oxford Radiocarbon Accelerator Unit, Research Laboratory for Archaeology and the History of Art, Oxford University, Oxford, United Kingdom.
[6]Museum of Natural History, Department of Prehistory, Vienna, Austria.
[7]University of Vienna, Department of Prehistory and Medieval Archaeology, Vienna, Austria.

Proceedings of the 6th International Radiocarbon and Archaeology Symposium, edited by E Boaretto and N R Rebollo Franco
RADIOCARBON, Vol 54, Nr 3–4, 2012, p 407–422

signals of the eruption in independently dated archives such as unusual tree rings (LaMarche and Hirschboeck 1984; Baillie and Munro 1988; Salzer and Hughes 2007; Baillie 2010) and sulfate peaks in ice cores (Vinther et al. 2006; Denton and Pearce 2008) and in stalagmites (Frisia et al. 2008). The archaeological evidence, on the other hand, favors an eruption date after the beginning of the New Kingdom in Egypt, which places the Thera eruption around 1500 BC (Bietak and Höflmayer 2007), or somewhat earlier, perhaps around 1530 BC (Warren 2009). In particular, not a single piece of Thera pumice out of over 400 samples appeared in any archaeological context before the 18th Dynasty or before the Late Bronze Age. This is surprising given the number of examined samples and the good quality of Thera pumice for use as abrasion material in workshops (Bietak 2012). Thus, ^{14}C dates the Thera eruption about 100 yr earlier than the archaeological evidence linked to the Egyptian historical chronology.

A similar disagreement of about 100 yr occurs between the ^{14}C dates from the stratigraphic sequence of the Tell el-Daba (also written "el-Dab^{c}a" or "el-Dab'a") excavation in the Nile Delta (Bietak and Höflmayer 2007), when the latter is linked to the Egyptian chronology. This difference has been discussed for several years, but never published, because the authors of this work had hoped that an explanation for the discrepancy would emerge. This may still happen, but for the time being it is an impasse (Bruins 2010), and it is therefore considered appropriate that the complete Tell el-Daba ^{14}C results are reported. We hope that in this way the community interested in the absolute chronology of the Late Bronze Age will be able to assess the situation more closely, and perhaps derive a solution for cutting this Gordian knot.

THE TELL EL-DABA SITE

The Tell el-Daba site is located in the southeastern part of the Nile Delta (Figure 1). In ancient times, the site was connected to the Mediterranean Sea by the Pelusiac Nile branch (Bietak 1975; Tronchère et al. 2008), which may have given it considerable strategic importance.

An overview of the Tell el-Daba area is shown in Figure 2, where the individual excavation sites are marked (Bietak et al. 2009). One of the challenging tasks was to establish a general stratigraphic sequence from the various excavation sites covering different, but largely overlapping, time periods. Contemporary phases at the different excavation sites were mainly identified by ceramic seriation, the introduction of new building materials and specific architectural features, and in a certain horizon the sudden occurrence of emergency graves. The result of these efforts are summarized in Figure 3 (Bietak and Höflmayer 2007), which shows both the phases of the individual excavation sites and the general phases in the rightmost column. Significant for establishing an absolute chronology for the Tell el-Daba general phases are the 2 datum lines on the far right representing links to the Egyptian historical chronology (Figure 3). A clear hiatus and abandonment of the Tell el-Daba site was identified with the beginning of the New Kingdom (Ahmose), resulting in the datum line at ~1530 BC. The datum line at ~1868 BC is from an inscription on a stela describing the 5th year of the reign of Sesostris III, thus providing a link to the Middle Kingdom. The latest phase C/2 can be dated by a series of scarabs from a workshop with the royal names of Ahmose, Ahmose-Nofretari, Amenhotep I, Thutmose III, and Amenhotep II with a *terminus ad quem* of Amenhotep II (~1427–1401 BC). Recently, a series of seals of the Hyksos King Khayan (~1600–1580 BC) was found in phases of the late E/1/early D/3 (15th Dynasty), as well as a fragment with cuneiform script indicating a possible link to the late Babylonian Kingdom around 1600–1550 BC (Bietak et al. 2009).

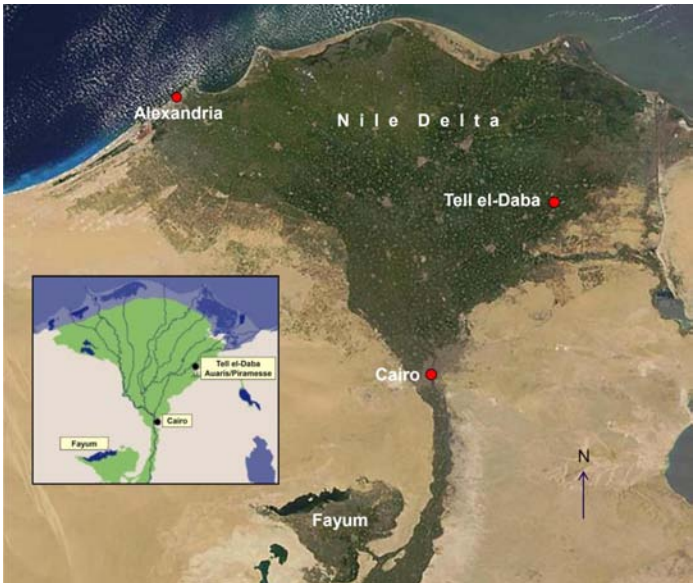

Figure 1 Satellite picture of the Nile Delta as it borders on the Mediterranean Sea (large figure). The Tell el-Daba site is located to the northeast of Cairo. The inset shows the approximate extent of the delta during the Bronze Age, with many branches of the Nile extending through the delta to the sea. Two ancient cities were identified at the Tell el-Daba site: the Hyksos capital of Avaris and the Rameses II city of Piramesse.

Figure 2 Overview of the Tell el-Daba area with an overlay of the ancient Pelusiac branch of the Nile (Bietak et al. 2009). The Pelusiac branch, like many of the other ancient Nile branches (see Figure 1 inset), has long disappeared, but was eventually identified by Bietak (1975) and Tronchère et al. (2008). Individual excavation areas are marked with capital letters/Roman numerals: Areas R/I, FI, FII, A/I-IV, A/V, and H/I-VI are summarized in Figure 3.

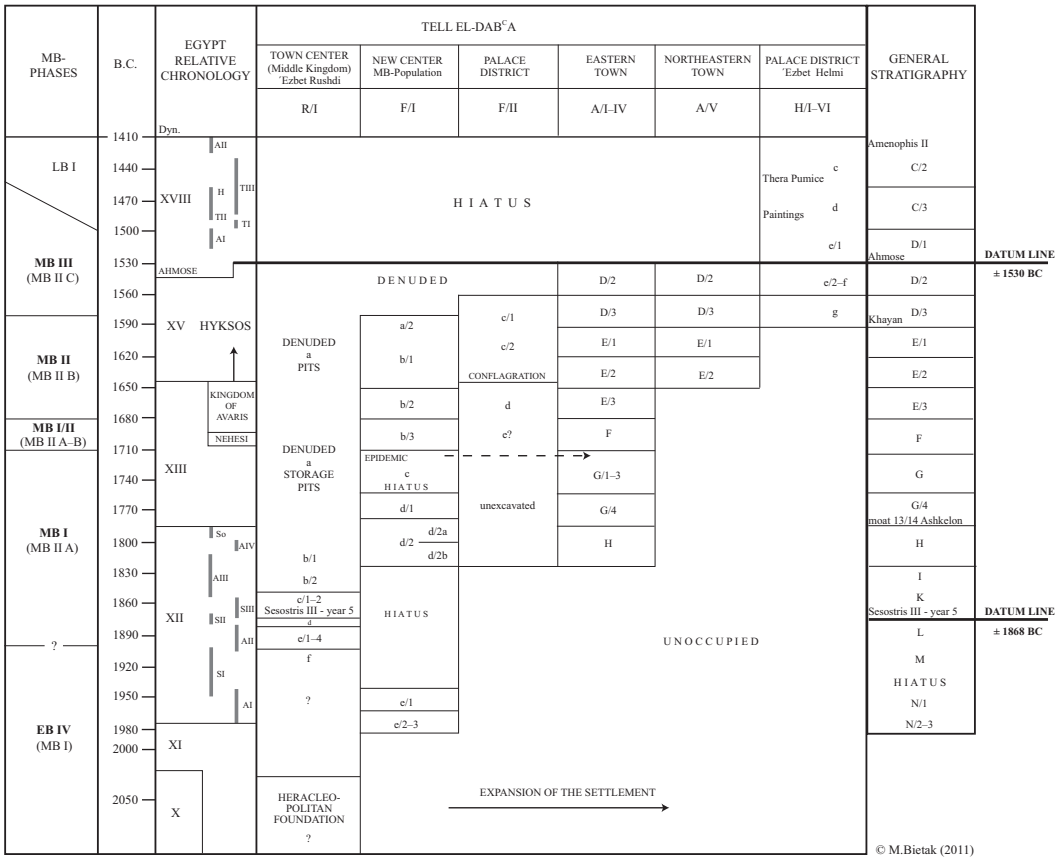

Figure 3 The figure is adapted from Bietak and Höflmayer (2007) after new excavation results in 2011. The general phases of Tell el-Daba as depicted in the rightmost column stems from 6 individual excavation sites that overlap (columns 4 to 9). The timescale in the second column was established from the historical sequence of dynasties and pharaohs (third column). The whole sequence of general phases is linked to the Egyptian historical chronology by 2 datum lines indicated at the far right of the figure: The abandonment of Avaris was supposedly caused by the conquest of Ahmose (~1530 BC), and the date of the construction of the Temple of Ezbet Rushdi (Phase K) from a stela from the 5th year of the reign of Sesostris III (~1868 BC). The left-most column gives the periods extending from the Early Bronze to Late Bronze Age.

Construction of the general phases comprises the archaeological backbone of the Tell el-Daba chronology covering the time period from about 2000 to 1400 BC. As it is a compound stratigraphy derived from different excavation areas with largely overlapping individual stratigraphies, it was important to compare the stratigraphy with ^{14}C measurements on samples assigned to the different phases. In order to reduce uncertainties inherent to the ^{14}C method (e.g. old-wood effect), only short-lived plant material was selected. Finally, only seeds of various plants were used that were found in the respective phases. There is, of course, always the question of a "secure context" for the samples. Even though the assignment of the samples to a particular phase was made with the best possible archaeological knowledge, one can never be absolutely certain about such assignments. For example, redundant plant seeds produced upwards from ancient pits or foundation ditches cannot be recognized. Therefore, samples from as many phases as possible were selected, assuming that at least a large fraction of them should be representative of the phases where they were found. Thus, the overall picture emerging from this process was considered to be more relevant than samples of individual phases. What is most important, is the fact that the relative chronology of the ^{14}C results described below confirms the overall sequence of phases.

RADIOCARBON MEASUREMENTS

A total of 47 seed samples were measured from Tell el-Daba at the VERA AMS facility of the University of Vienna. Sample selection, sample preparation, accelerator mass spectrometry (AMS) measurement, and calibration were the crucial steps in this procedure.

Sample Selection

We decided to use only short-lived seed samples for ^{14}C dating. Only annual grasses (Poaceae) from samples exhibiting no signs of disturbance were selected for analysis. The latter condition was verified by the absence of microscopic abnormalities in the matrix from which the seeds were recovered. Only charred material from archaeological settings was selected, i.e. the result of human activity, which makes it unlikely that the material was transported by Nile water from other locations. In addition, careful considerations about the provenance of the samples with respect to particular phases were employed.

Sample Preparation

Sample preparation procedures of the VERA laboratory (Wild et al. 2008) were used to extract carbon from the seeds, which was then pressed into aluminium target holders of our 40-sample multicathode source of negative ions by Cs sputtering (MC-SNICS). Sample preparation was performed by applying acid-base-acid treatment to remove carbonates and humic acids, combustion of the pretreated sample with CuO at 900 °C, and reduction of the thus-produced CO_2 to graphite at 610 °C with H_2 and an Fe catalyst according to the method developed by Vogel et al. (1984).

AMS Measurements

^{14}C measurements were performed by sequential injection of ^{12}C, ^{13}C, and ^{14}C into the tandem operated at a terminal voltage of 2.7 MV. After terminal gas stripping with O_2, 3+ ions were selected by the high-energy 90° analyzing magnet. $^{12}C^{3+}$ and $^{13}C^{3+}$ ion currents were measured in offset Faraday cups after the magnet and $^{14}C^{3+}$ ions were counted in a silicon surface barrier detector after complete clean-up of background ions with a 90° high-resolution electrostatic analyzer. $^{14}C/^{12}C$ and $^{13}C/^{12}C$ isotopic ratios were normalized to calibration targets prepared from IAEA reference material with known carbon isotope contents, measured together with the Tell el-Daba samples. The precision of ^{14}C measurements at VERA has continuously improved and has reached levels between 25 to 35 ^{14}C yr (Steier et al. 2004; see also Table 1). In special cases, this has been pushed to even higher precision of 15 to 25 ^{14}C yr (Dellinger et al. 2004).

Calibration

Uncalibrated ^{14}C ages were calculated according to standard procedures (Stuiver and Polach 1977), and then converted into calibrated calendar dates with the OxCal computer program (Bronk Ramsey 2009a,b) using the IntCal09 calibration curve (Reimer et al. 2009).

Summary of ^{14}C Results

The results of the ^{14}C measurements are summarized in Table 1. Out of a total of 47 samples, 40 could be firmly assigned to specific phases of Tell el-Daba. They are listed in Table 1a. In order to check for a possible laboratory bias, splits of 5 samples were measured independently at the Oxford Radiocarbon Accelerator Unit, with their results also listed in Table 1a. The ^{14}C ages from Oxford agree with the Vienna ones within the 1σ uncertainties, except for one (OxA-15901), which shows a 2σ deviation. Thus, a laboratory bias can be excluded. In addition to the ABA-treated samples,

Table 1a Results of ^{14}C measurements on short-lived samples from Tell el-Daba.

Tell el-Daba general phase	AMS nr	Lab code	Material	$\delta^{13}C$ (‰)	^{14}C age[a] (yr BP)	Calibrated range[b] (BC)	Sequenced range[b] (BC)
C/2	AMS-25	VERA-3031	seeds, *Lolium* type	–21.0 ± 1.4	3414 ± 35	1875–1621	1667–1537
C/2-3	AMS-48	VERA-3724	seeds, *Lolium* type	–21.4 ± 0.5	3320 ± 29		
		OxA-15959		–23.4 ± 0.3	3296 ± 31		
		OxA-15957		–22.4 ± 0.3	3322 ± 31		
		weighted mean			3313 ± 17	1636–1525	1665–1543
		OxA-15958[c]		–22.4 ± 0.3	3287 ± 33		
C/2-3	AMS-49	VERA-3725	seed, *Lolium* type	–26.3 ± 0.5	3336 ± 29	1726–1527	1668–1546
D/1	AMS-26	VERA-3032	seed, *Lolium* type	–22.9 ± 1.2	3314 ± 36	1687–1511	1688–1601
D/2	AMS-28	VERA-3616	seeds, Poaceae	–24.5 ± 0.6	3337 ± 44	1739–1516	1723–1630
D/2	AMS-13	VERA-2628	seed, *Triticum* sp., Poaceae	–22.6 ± 0.5	3359 ± 34	1741–1533	1698–1631
D/2	AMS-12	VERA-2627	seed, *Lolium* type	–21.7 ± 0.5	3390 ± 34	1863–1562	1722–1633
D/2	AMS-46	VERA-3622	seeds, Poaceae	–21.0 ± 0.6	3394 ± 36	1869–1541	1722–1633
D/2	AMS-39	VERA-3621	seeds, *Lolium* type	–22.0 ± 0.5	3354 ± 26		
		OxA-15953		–22.4 ± 0.3	3392 ± 31		
		OxA-15901		–22.9 ± 0.3	3479 ± 33		
		weighted mean			3399 ± 37	1873–1609	1708–1633
		OxA-15979[c]		–22.9 ± 0.3	3383 ± 30		
		OxA-15980[c]		–22.6 ± 0.3	3392 ± 31		
D/3-D/2	AMS-45	VERA-3645	seeds, *Lolium* type, Poaceae	–21.8 ± 0.6	3351 ± 38	1739–1529	1731–1656
D/3	AMS-37	VERA-3620	seeds, *Lolium* type	–23.0 ± 0.5	3377 ± 33	1751–1537	1738–1673
D/3	AMS-14	VERA-2629	seeds, *Lolium* type, Poaceae	–22.1 ± 0.6	3384 ± 30	1752–1609	1738–1674
D/3	AMS-36	VERA-3619	seeds, *Lolium* type	–22.9 ± 0.5	3396 ± 34	1866–1610	1739–1674
D/3	AMS-18	VERA-2895	seed, *Lolium* type	–13.3 ± 0.9	3426 ± 26	1873–1640	1741–1681
D/3	AMS-19	VERA-2896	seeds, Poaceae	–21.0 ± 0.7	3428 ± 37	1878–1633	1741–1677
D/3	AMS-27	VERA-3033	seed, Cerealia	–22.0 ± 1.9	3480 ± 28	1886–1700	1745–1682
E/1	AMS-11	VERA-2626	seed, *Lolium* type, *Lolium/Bromus/Agropyron* sp.	–22.8 ± 0.5	3389 ± 36	1863–1539	1754–1693
E/1	AMS-29	VERA-3617	seeds, Poaceae	–24.4 ± 0.5	3422 ± 35	1877–1627	1756–1694
E/1	AMS-31	VERA-3636	seeds, *Lolium* type	–25.0 ± 0.6	3449 ± 26	1878–1689	1757–1694
E/1	AMS-30	VERA-3618	seeds, Cerealia	–22.8 ± 0.5	3436 ± 35		
		OxA-15949		–23.7 ± 0.3	3437 ± 30		
		OxA-15948		–22.9 ± 0.3	3511 ± 32		
		weighted mean			3462 ± 25	1881–1693	1759–1694
E/2	AMS-33	VERA-3637	seeds, *Lolium* type	–23.4 ± 0.4	3415 ± 26	1864–1633	1781–1702
E/3	AMS-20	VERA-2897	seeds, *Hordeum vulgare*	–17.0 ± 0.8	3525 ± 26	1931–1767	1846–1747

Table 1a Results of ^{14}C measurements on short-lived samples from Tell el-Daba. *(Continued)*

Tell el-Daba general phase	AMS nr	Lab code	Material	δ^{13}C (‰)	^{14}C age[a] (yr BP)	Calibrated range[b] (BC)	Sequenced range[b] (BC)
F-E/3	AMS-43	VERA-3643	seeds, Poaceae	–22.3 ± 0.5	3450 ± 26	1878–1689	1863–1755
F	AMS-10	VERA-2625	seeds, *Lolium* sp., *Lolium* type, *Lolium/Bromus* sp.	–21.3 ± 0.5	3467 ± 35	1886–1691	1870–1767
F	AMS-21	VERA-2898	seeds, *Lolium* type, *Phalaris/Cynodon* sp.	–16.9 ± 0.6	3505 ± 27	1904–1747	1871–1770
G/1-3	AMS-42	VERA-3642	seeds, *Lolium* type, Poaceae	–21.3 ± 0.4	3447 ± 25	1877–1689	1884–1802
G/1-3	AMS-08	VERA-2623	seeds, *Triticum dicoccum*	–19.6 ± 0.5	3466 ± 39	1887–1690	1886–1802
G/1-3	AMS-07	VERA-2622	seeds, *Lolium* type, Poaceae	–21.6 ± 0.5	3481 ± 36	1896–1692	1887–1803
G/1-3	AMS-09	VERA-2624	seeds, *Hordeum vulgare*, *Lolium* type	–19.9 ± 0.4	3530 ± 34	1947–1753	1894–1802
G/4	AMS-40	VERA-3640	seeds, *Lolium* type	–23.8 ± 0.5	3530 ± 38		
		OxA-15956		–23.3 ± 0.3	3504 ± 32		
		OxA-15954		–23.1 ± 0.3	3532 ± 34		
		weighted mean			3521 ± 20	1917–1771	1920–1832
		OxA-15981[c]		–23.3 ± 0.3	3570 ± 30		
		OxA-15955[c]		–22.7 ± 0.3	3530 ± 32		
G/4	AMS-22	VERA-2899	seeds, Poaceae	–20.4 ± 1.0	3591 ± 26	2024–1886	1928–1867
H	AMS-34	VERA-3638	seeds, *Lolium* type	–23.7 ± 0.5	3522 ± 37	1946–1746	1942–1884
H	AMS-35	VERA-3639	seeds, *Lolium* type	–22.7 ± 0.4	3553 ± 25		
		OxA-15951		–24.0 ± 0.3	3522 ± 32		
		OxA-15952		–22.8 ± 0.3	3577 ± 32		
		weighted mean			3551 ± 17	1949–1781	1940–1886
		OxA-15950[c]		–22.2 ± 0.3	3490 ± 32		
		OxA-15978[c]		–23.3 ± 0.3	3589 ± 32		
H	AMS-03	VERA-2618	seed, *Lolium* type	–21.0 ± 0.4	3593 ± 34	2112–1828	1946–1886
M	AMS-16	VERA-2631	seeds, Cerealia, *Lolium* type	–23.7 ± 0.6	3643 ± 35	2135–1917	2124–1972
N/1	AMS-05	VERA-2620	seed, *Lolium* type, Poaceae	–22.7 ± 0.4	3688 ± 36	2197–1963	2141–2021
N/1	AMS-04	VERA-2619	seed, *Lolium* type, Poaceae	–22.8 ± 0.4	3697 ± 37	2201–1975	2143–2022
N/2-3	AMS-24	VERA-2901	seeds, Poaceae	–17.8 ± 0.6	3725 ± 30	2204–2032	2197–2042
N/2-3	AMS-41	VERA-3641	seeds, *Lolium* type	–21.9 ± 0.8	3739 ± 38	2281–2031	2198–2041
N/2-3	AMS-23	VERA-2900	seeds, *Lolium* type	–15.8 ± 0.7	3755 ± 26	2281–2043	2198–2043

[a] 1σ uncertainty.

[b] Probability ranges (95.4%) determined with the OxCal v 4 program and IntCal09 calibration curve.

[c] Humic acids (see text).

humic acids extracted from the samples were also measured at the Oxford lab and listed in Table 1a. It is important to note that in those cases where a sufficient yield of humic acids for ^{14}C measurements existed (4 out of 5 samples), the ^{14}C ages agreed within 1σ uncertainty with those of the fully ABA-pretreated samples. This indicates a significant integrity of the samples, essentially excluding any contamination by humic acids from the environment. For the calibration and Bayesian sequencing of the sample splits, we used the weighted average of the VERA results and the respective ABA-treated Oxford results as indicated in Table 1. For completeness, the ^{14}C results of the remaining 7 samples with uncertain phase assignments are also listed (Table 1b).

Table 1b Results of ^{14}C measurements on short-lived samples from Tell el-Daba, whose provenance is unclear and/or disturbed.

Tell el-Daba general phase	AMS nr	Lab code	Material	$\delta^{13}C$ (‰)	^{14}C age[a] (yr BP)	Calibrated range[b] (BC)
C/3	AMS-17	VERA-2632	seeds, Poaceae	–22.7 ± 0.5	3424 ± 31	1876–1631
D/2-D/1	AMS-15	VERA-2630	seed, Poaceae	–22.7 ± 0.6	3345 ± 31	1733–1530
D/2-D/1	AMS-47	VERA-3623	seeds, *Lolium* type	–22.6 ± 0.4	3356 ± 23	1737–1537
G/1-3	AMS-44	VERA-3644	seeds, *Lolium* type	–23.9 ± 0.5	3641 ± 36	2135–1911
H (?)	AMS-06	VERA-2621	seed, *Triticum* sp., *Lolium* type	–22.3 ± 0.5	3493 ± 34	1910–1698
H or N/1	AMS-01	VERA-2616	seed, Poaceae	–23.1 ± 0.5	3610 ± 37	2125–1883
N/1-3 (?)	AMS-02	VERA-2617	seed, *Lolium* type, Poaceae	–19.7 ± 0.5	3433 ± 38	1880–1637

[a] 1σ uncertainty.

[b] Probability ranges (95.4%) determined with the OxCal v 4 program and IntCal09 calibration curve.

DISCUSSION

The Tell el-Daba Results

As described above, an absolute timeframe of general phases of the Tell el-Daba site was established through links to the Egyptian historical chronology (Figure 3). Archaeological characterization of the phases within the larger context of cultural exchanges in the east Mediterranean can then, in principle, provide a synchronization of other civilizations in the east Mediterranean in the 2nd millennium BC. It is useful for such far-reaching conclusions that the chronological framework is compared with an independent method. This was the purpose of the ^{14}C measurements. In Figure 4, the general phases are displayed according to the Egyptian historical chronology, both in horizontal and vertical direction.

The diagonal line in the figure indicates where the ^{14}C dates would fall, if there is an agreement between the ^{14}C dates and the historical chronology of Egypt. It is evident that the calibrated 95.4% probability ranges of the ^{14}C dates are shifted to one side, indicating older ages.

We used a simple Bayesian model to calculate the probability distribution of an assumed constant age offset, which would be needed to obtain agreement between the (unsequenced) ^{14}C results of Figure 4 and the archaeological-historical dates. The resulting distribution shows an age offset centering at 120 yr, with negligible probability for offsets smaller than 100 yr (Figure 5). This large age shift cannot be explained by the small seasonal offset of (19 ± 5) ^{14}C yr found by dating material of known age from Egypt (Dee et al. 2010).

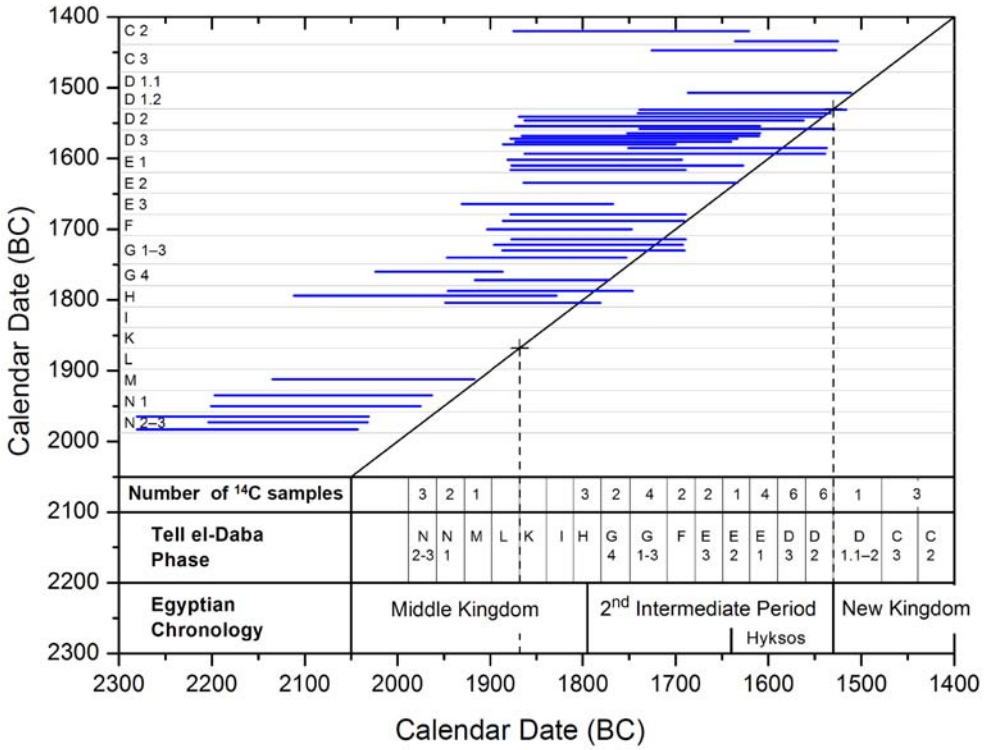

Figure 4 Comparison of the calibrated ^{14}C dates (95.4% probability ranges) of samples from the respective Tell el-Daba phases, which in turn are arranged according to the historical chronology of Egypt on both axes. The dashed vertical lines indicate the links of the Tell el-Daba phases to the Egyptian chronology (see Figure 3). For an agreement between ^{14}C dates and the chronology of the Tell el-Daba phases, the former should scatter along the diagonal line, which they obviously do not. The ^{14}C dates are clearly shifted towards older ages.

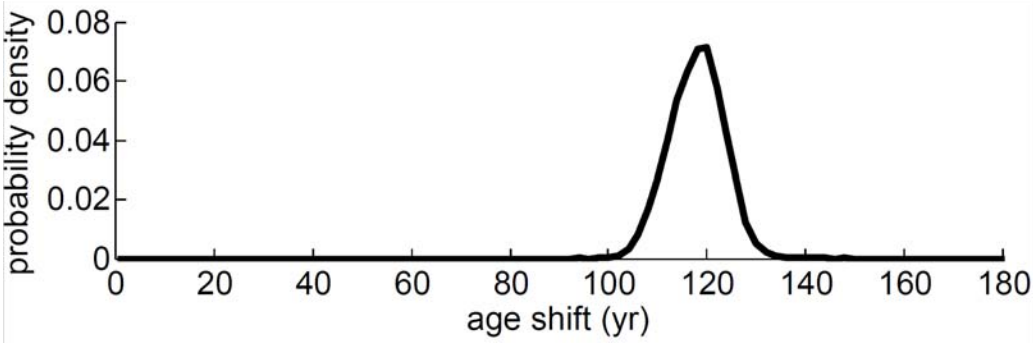

Figure 5 Posterior probability distribution for the age shift of ^{14}C data in Tell el-Daba

Accepting that the phases are in the correct chronological order, and that the samples do belong to the respective phases, one can apply Bayesian sequencing (Bronk Ramsey 2009a,b), which considerably reduces the uncertainties. Figures 6a and 6b display the results of the OxCal calibration with Bayesian sequencing including the option to recognize outliers.

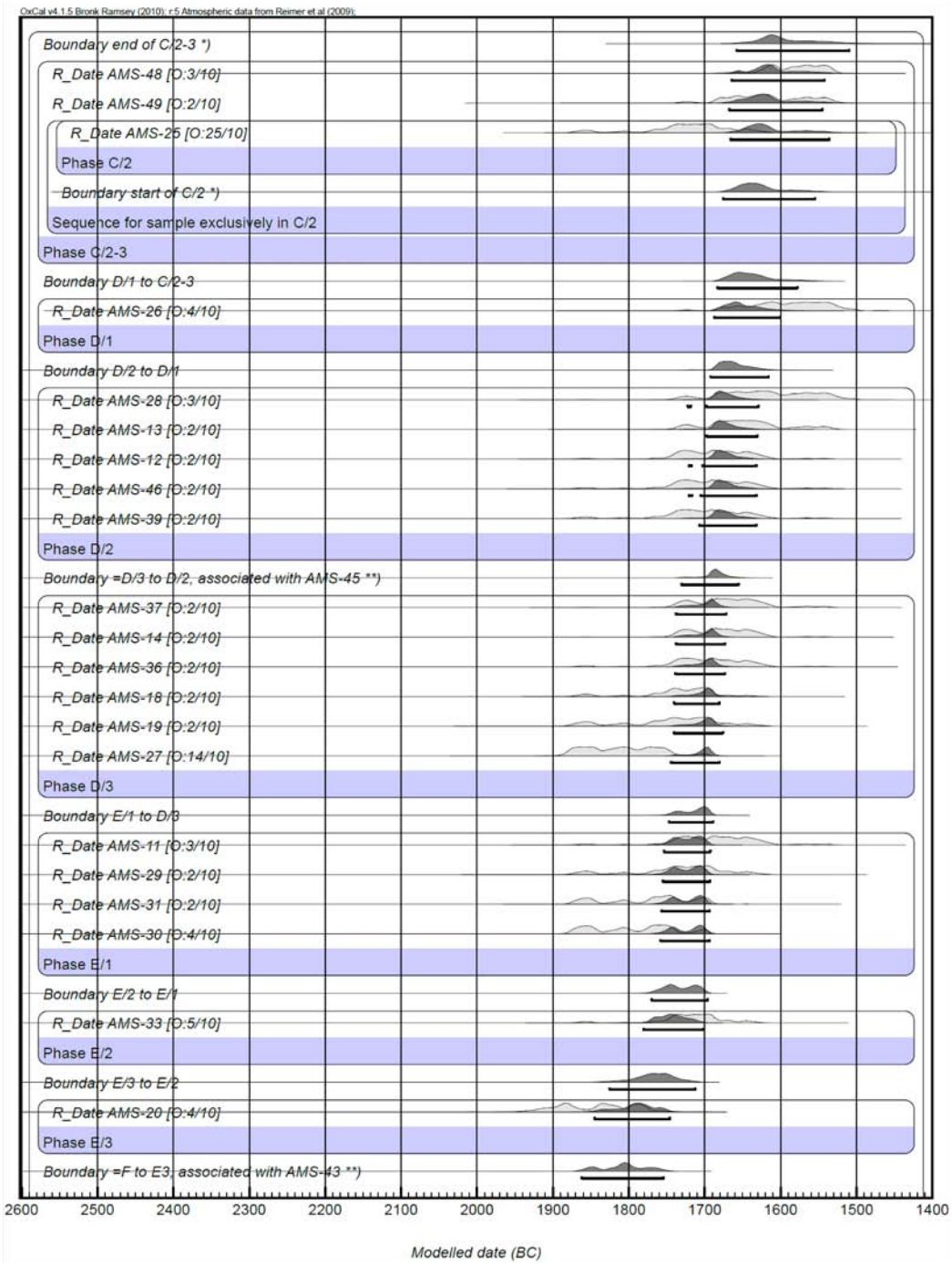

Figure 6a Bayesian sequencing (continued in Figure 6b) of the ^{14}C dates assigned to the respective Tell el-Daba phases (see Figures 3 and 4). The light gray curves give the single-sample calibration distributions, whereas the dark curves give the modeled posterior distributions. Calculation was performed using OxCal v 4.1.5 (Bronk Ramsey 2009a,b). Note that for consistency with Figures 3, 4, and 6, the phases are arranged in stratigraphical order. Thus, chronologically the sequence starts at the bottom of Figure 6b and ends at the top of Figure 6a.

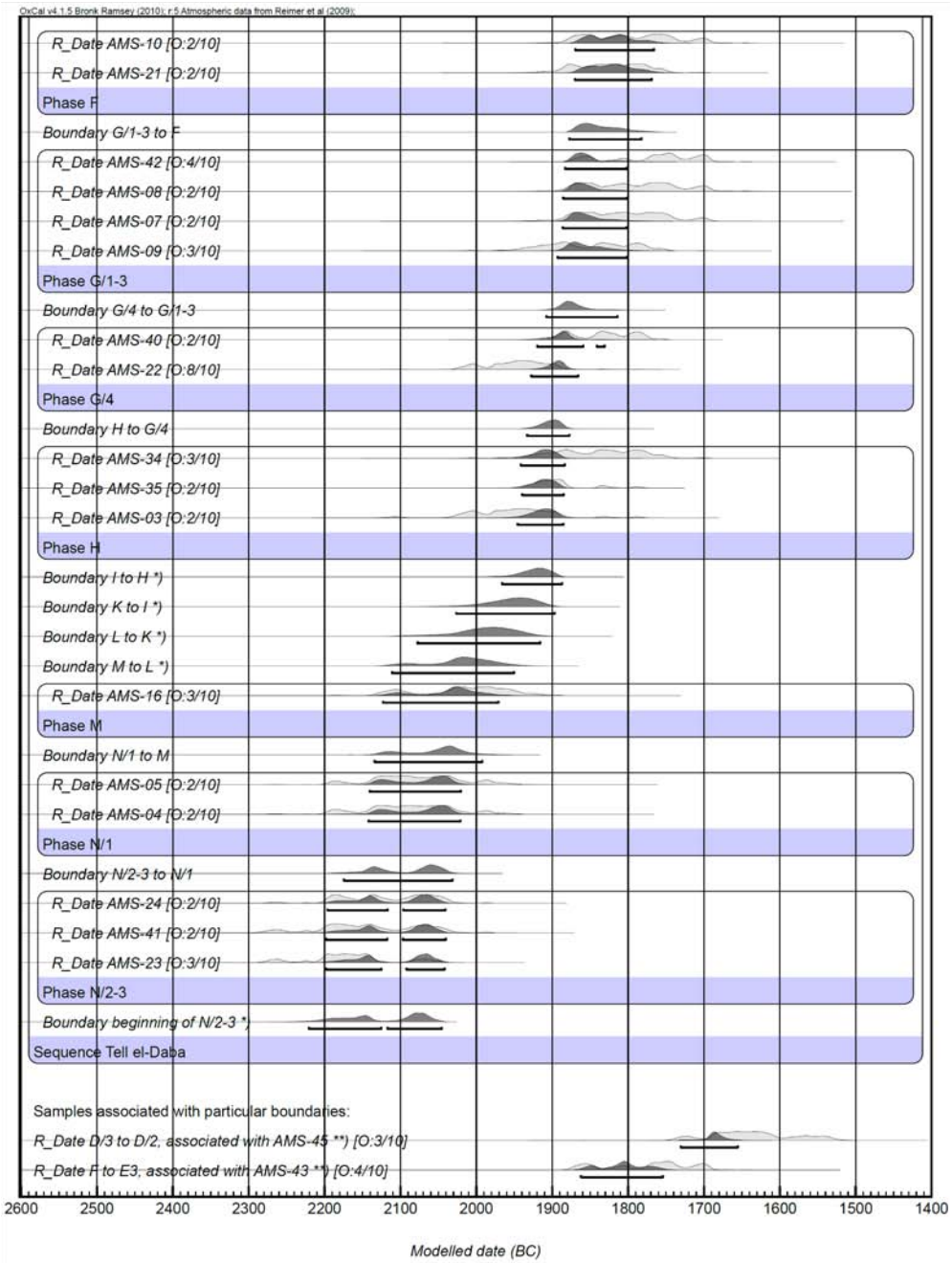

Figure 6b Second half of the Bayesian sequencing results. For details, see the caption of Figure 6a. * Results for boundaries marked with a single asterisk are not bracketed by samples and are therefore just rough estimates, which cannot be used for rigorous conclusions. ** Double asterisks mark the 2 samples that are stratigraphically located at phase transitions (AMS-45 at the D/3 to D/2 boundary, and AMS-43 at the F to E3 boundary). In these cases, the model identifies the posterior distribution for the boundary with that of the corresponding sample. The results for these 2 samples are plotted separately at the bottom of Figure 6b.

The first number in the square brackets of Figures 6a and 6b give the percentage probability for the sample to be an outlier; the second number gives the starting value. For example, for AMS-25 in the 4th line one finds 25%, whereas most samples are at the 2 to 4% level, which means that the applied model agrees very well with the measured data.

Comparison of Tell-el-Daba Results with Recent ^{14}C Dating of the Egyptian Dynastic Period and the Santorini Results

Compared to the single-calibration results of Figure 4, the shift in ^{14}C dates becomes more pronounced for the sequenced results shown in Figure 7. In this figure, the dotted line represents the constant 120-yr shift calculated above (cf. Figure 5). This shift is of great concern to both archaeologists and ^{14}C dating scientists because it signifies a serious disagreement between the 2 well-established methods.

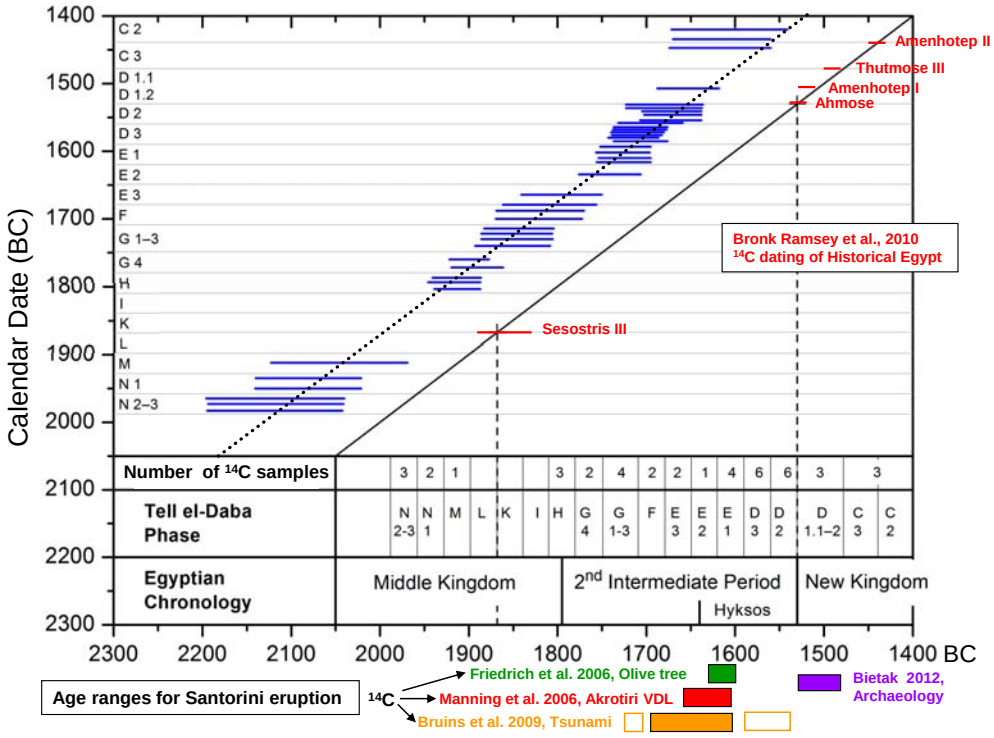

Figure 7 Comparison of the sequenced ^{14}C results (95.4% probability ranges) with the Tell el-Daba phases (see Figure 4 caption for details of the display). The dotted line corresponds to the constant time shift of 120 yr calculated for Figure 5. Also plotted in the figure are results from the recent ^{14}C dating of the dynastic period of Egypt (red lines; Bronk Ramsey et al. 2010). On the bottom of the figure, below the time axis, the 95.4% age ranges of the ^{14}C dating of the Santorini eruption (colored boxes: Friedrich et al. 2006; Manning et al. 2006; Bruins et al. 2009) are compared with the eruption range from archaeological considerations (violet box: Bietak 2012). This figure is displayed in color in the online edition of the article.

It is possible to compare the Tell el-Daba results with other ^{14}C data falling into the same time period. In Figure 7, the ^{14}C dates for the ascension of specific kings in the New Kingdom (Bronk Ramsey at al. 2010) are displayed and obviously agree well with the historical chronology in the New Kingdom, since they all fall on the diagonal line. Unfortunately, there are no data available from this investigation for the 2nd Intermediate Period, where most of the ^{14}C measurements (75%)

at Tell el-Daba were performed. However, the historical date of Sesostris III in the Middle Kingdom is again well reproduced by the Oxford ^{14}C data (Bronk Ramsey et al. 2010).

Below the horizontal time axis in Figure 7, we display the ^{14}C results for the outermost tree ring of the olive tree buried in the Santorini eruption (Friedrich et al. 2006) and for the volcanic destruction layer of Santorini established by Manning et al. (2006). The somewhat less precise ^{14}C dates for cattle bones found in the tsunami deposits on Palaikastro of Crete (Bruins et al. 2008, 2009) are also displayed. All 3 ^{14}C results point to a Santorini eruption date in the second half of the 17th century BC. In contrast to these results, the archaeological evidence linked to the Egyptian historical chronology puts the Santorini eruption after the beginning of the New Kingdom, i.e. ~1530 BC or later (Bietak 2012). This indicates a similar shift in time as the ^{14}C dates from Tell el-Daba itself.

Attempts for a Solution of the Dating Dilemma

It is clear from Figure 7 that there is a serious disagreement between the Tell el-Daba archaeological-historical chronology and the ^{14}C dating results. Since a good agreement has been found between the ^{14}C dates of short-lived organic material directly linked to the Egyptian historical chronology (Bronk Ramsey et al. 2010), a general offset of the order of 100 yr for ^{14}C dates in Egypt can be ruled out. The seasonal growth effect in Egypt of (19 ± 5) ^{14}C yr, explored by the Oxford group (Dee et al. 2010), cannot explain this shift. The Tell el-Daba samples are from seed material of plants that grow above ground, and take up CO_2 from the air. A general contribution of the so-called hardwater effect, i.e. the incorporation of carbon depleted in ^{14}C from water into plants through the roots, has either not been observed (Tauber 1983) or is very small (Ford et al. 2007). Even if there would be some dead-carbon uptake from water causing the 120-yr shift, it would probably also have appeared in the Oxford measurements (Bronk Ramsey et al. 2010), because essentially all freshwater in Egypt is supplied by the Nile. Since this is not the case, it is unlikely that only the Tell el-Daba site would show such a shift. It should be noted, however, that during winter most of the water originates from the White Nile, whereas during the summer more of the water is supplied by the Blue Nile. In addition, during the 2nd millennium BC Tell el-Daba was located only 30 km from the Mediterranean coast with the possibility of seawater filling the empty Nile channels, allowing ships from Tell el-Daba to reach the sea even during the dry season (January to June). Although these complex conditions make it difficult to draw quantitative conclusions on the absence or presence of dead carbon in water at Tell el-Daba, it seems not very likely that it would affect the ^{14}C results by the amount required to explain the 120-yr shift. More studies on the effect of upwelling and uptake of carbon by the roots in the northern delta region would be necessary to ultimately clarify this situation. On more general ground, extensive studies were performed by Manning et al. (2010) and Manning and Kromer (2011, 2012) on possible ^{14}C offsets in the Aegian-Anatolean-east Mediterranean region, finding a weighted average offset with respect to the IntCal09 calibration (Reimer et al. 2009) of (0.75 ± 1.73) ^{14}C yr, i.e. essentially zero.

The observed difference between ^{14}C dates of the Santorini eruption and the archaeological expectation of the event is again coupled to the Tell el-Daba stratigraphy and its links to the Egyptian historical chronology. It is well known that volcanic vents exhale CO_2 depleted in ^{14}C (e.g. Bruns et al. 1980; Pasquier-Cardin et al. 1999), but it is also known that this effect disappears a few hundred meters from the vent. Both the olive tree (Friedrich et al. 2006) and samples from the volcanic destruction layer in Akrotiri (Manning et al. 2006) grew far away from known volcanic vents; therefore, a dead carbon contribution is unlikely for these samples. In addition, many samples in the investigation of Manning et al. (2006) came from surrounding islands with no volcanic activity. The material from Crete (Bruins et al. 2008, 2009) should also not have been affected by volcanic CO_2.

Other Check Points of ^{14}C Dates and the Archaeological-Egyptian Timescale

Recently, the Late Bronze Age shipwreck of Uluburun off the south coast of Turkey was investigated by combining ^{14}C dating and dendrochronology (Manning et al. 2009b). With this approach, the last voyage of this ship was determined to have occurred around 1320 ± 15 BC (Manning et al. 2009b). This date is consistent with the find of a scarab from Nefertiti in the shipwreck, since her husband king Akhenaten (Echnaton, Amenhotep IV) reigned from 1352 to 1336 BC (Shaw 2000). Recent ^{14}C measurements of samples from the Amarna period agree well with the historical Egyptian chronology (Bronk Ramsey et al. 2010). Preliminary results from Bayesian sequencing of ^{14}C dates from the well-established stratigraphic excavation in Aegina Kolonna on an island 50 km south of Athens are inconclusive as to whether there exists an offset between the historical chronology and the ^{14}C data (Wild et al. 2010). According to the ^{14}C data, the beginning of the Middle Helladic I period (MHI) is concordant with the historical chronology, whereas in the LHI/II part of the sequence the ^{14}C data may indicate a shift to older ages and may thus favor the science-based chronology. However, the latter results need verification by additional ^{14}C dates.

CONCLUSION

^{14}C dating has come of age and now contributes significantly towards establishing an absolute timescale in the ancient history of the east Mediterranean. While the direct comparison of ^{14}C dating with dynastic Egypt led to a good agreement with the historical Egyptian chronology (Bronk Ramsey et al. 2010), there are serious discrepancies at places where the absolute timescale of an archaeological excavation has been established by specific links to the Egyptian chronology. Tell el-Daba is clearly one of these places, but a similar disagreement exists for the date of the Santorini eruption. In this work, it is argued that it is difficult to find uncertainties in ^{14}C dating that could explain a time shift of 100 yr or more. On the other hand, archaeology in the east Mediterranean is built up on numerous check points leading to a consistent network of relative chronologies across the whole area, and several links to the Egyptian historical chronology provide an absolute timeframe. Since for a deeper understanding of human activities in the ancient world of the east Mediterranean a synchronization of civilizations is very desirable, one should strive for a consensus between ^{14}C dating and archaeology. In this respect, it seems difficult to accept the view expressed by Bruins et al. (2009) that we have to live with 2 different chronologies (see also Bruins 2010).

The main difference between ^{14}C dating and archaeology can perhaps be summarized in the following way: Although the ^{14}C clock is based on a well-established physical law (radioactive decay), which is not affected by environmental conditions, it requires detailed knowledge of the starting conditions, i.e. the ^{14}C content of the sample before the clock starts running. Despite extensive efforts to establish global starting conditions for the time range of ^{14}C dating (Reimer et al. 2009), there sometimes remains the question of possible deviations from the calibration curve by regional effects. Although it seems unlikely that the 120-yr shift of Tell el-Daba can be explained by such a regional effect, on the basis of the current ^{14}C results it cannot be definitely excluded.

Archaeological dating, on the other hand, depends primarily on the seriation of pottery obtained from well-dated assemblages and the seriation at the site, where the changing market situation in specific phases is evaluated by the quantification of ceramic or metal types that occur in the same time context in repetitive proportions. In addition, dates can be determined by inscribed material such as names of pharaohs that are used as *termini post quos*. In lucky circumstances, one has datum lines like the 5th year of Sesostris III (the construction of the Temple of Ezbet Rushdi, beginning of Phase K) or the conquest of Avaris (end of phase D/2) at Tell el-Daba. Cross-dates with other better-dated contexts of the same type also play an important role.

In conclusion, the Tell el-Daba site offers a particularly challenging problem to establish an accurate absolute timeframe for the 2nd millennium BC. Finding a consensus between ^{14}C dating and archaeological-historical dating must be the goal for the future. No matter how sure we are about the respective results, there may still be hidden systematic effects we have not yet detected.

The project as a whole has been a very fruitful collaboration between scholars in the field of natural sciences and the humanities. If nothing else, we have learned to respect each other's efforts in searching for the truth. To eventually reach a consensus of these 2 approaches for our past is clearly a challenging task for the future.

ACKOWLEDGMENTS

This work was supported by the SCIEM 2000 project (The Synchronisation of Civilisations in the Eastern Mediterranean in the Second Millennium BC), a Special Research Program (SFB) of the Austrian Academy of Sciences and the Austrian Science Fund (FWF). Over the years, we have benefitted from many fruitful discussions with colleagues interested in this subject.

REFERENCES

Baillie MGI. 2010. Volcanoes, ice-cores and tree-rings: one story or two? *Antiquity* 84(323):202–15.

Baillie MGI, Munro AR. 1988. Irish tree rings, Santorini and volcanic dust veils. *Nature* 332(6162):344–6.

Balter M. 2006. New carbon dates support revised history of ancient Mediterranean. *Science* 312(5773):508–9.

Bietak M. 1975. Tell el-Daba II. Der Fundort im Rahmen einer archäologisch-geographischen Untersuchuing über das ägyptische Ostdelta. *Untersuchungen der Zweigstelle Kairo des Österreichischen Archäologischen Instituts, Bd. II. Denkschriften der Gesamtakademie der Österreichischen Akademie der Wissenschaften Bd. IV.* Vienna.

Bietak M. 2012. Antagonisms in historical and radiocarbon chronology. In: Shortland AJ, Bronk Ramsey C, editors. *Radiocarbon and the Chronologies of Ancient Egypt*. Oxford: Oxbow. In press.

Bietak M, Höflmayer F. 2007. Introduction: high and low chronology. In: Bietak M, Czerny E, editors. *The Synhronisation of Civilisations in the Eastern Mediterranean in the Second Millennium BC – III*. Vienna: Austrian Academy of Sciences. p 13–27.

Bietak M, Forstner-Müller I, van Koppen F, Radner K. 2009. Der Hyksos-Palast bei Tell el-Daba. Zweite und Dritte Grabungskampagne (Frühling 2008 und Frühling 2009). *Egypt and the Levant* 19:91–119.

Bronk Ramsey C. 2009a. Bayesian analysis of radiocarbon dates. *Radiocarbon* 51(1):337–60.

Bronk Ramsey C. 2009b. Dealing with outliers and offsets in radiocarbon dating. *Radiocarbon* 51(3):1023–45.

Bronk Ramsey C, Dee MW, Rowland JM, Higham TFG, Harris SA, Brock F, Quiles A, Wild EM, Marcus ES, Shortland AJ. 2010. Radiocarbon-based chronology for dynastic Egypt. *Science* 328(5985):1554–7.

Bruins HJ. 2010. Dating pharaonic Egypt. *Science* 328(5985):1489–90.

Bruins HJ, MacGillivray A, Synolakis CE, Benjamini C, Keller J, Kisch HJ, Klügel A, van der Plicht J. 2008. Geoarchaeological tsunami deposits at Palaikastro (Crete) and the Late Minoan IA eruption of Santorini. *Journal of Archaeological Science* 35(1):191–212.

Bruins HJ, van der Plicht J, MacGillivray JA. 2009. The Minoan Santorini eruption and tsunami deposits in Palaikastro (Crete): dating by geology, archaeology, ^{14}C, and Egyptian chronology. *Radiocarbon* 51(2): 397–411.

Bruns M, Levin I, Münnich KO, Hubberten HW, Fillipakis S. 1980. Regional sources of volcanic carbon dioxide and their influence on ^{14}C content of present-day plant material. *Radiocarbon* 22(2):532–6.

Dee MW, Brock F, Harris SA, Bronk Ramsey C, Shortland AJ, Higham TFG, Rowland JM. 2010. Investigating the likelihood of a reservoir offset in the radiocarbon record for ancient Egypt. *Journal of Archaeological Science* 37(4):687–93.

Dellinger F, Kutschera W, Nicolussi K, Schießling P, Steier P, Wild EM. 2004. A ^{14}C calibration with AMS from 3500 to 3000 BC, derived from a high-elevation stone-pine tree-ring chronology. *Radiocarbon* 46(2): 969–78.

Denton JS, Pearce NJG. 2008. Comment on "A synchronized dating of three Greenland ice cores throughout the Holocene" by B. M. Vinther et al.: no Minoan tephra in the 1642 B.C. layer of the GRIP ice core. *Journal of Geophysical Research* 113: D04303.

Ford CR, Wurzburger N, Hendrick RL, Teskey RO. 2007. Soil DIC uptake and fixation in *Pinus teada* seedlings and its C contribution to plant tissues and ectomycorrhizal fungi. *Tree Physiology* 27(3):375–83.

Friedrich WL, Kromer B, Friedrich M, Heinemeier J, Pfeiffer T, Talamo S. 2006. Santorini eruption radiocarbon dated to 1627–1600 B.C. *Science* 312(5773):548.

Friedrich WL, Kromer B, Friedrich M, Heinemeier J, Pfeiffer T, Talamo S. 2009. Santorini eruption radio-

carbon dated to 1627–1600 BC: further discussion. In: Manning SW, Bruce MJ, editors. *Tree-Rings, Kings, and Old World Archaeology and Environment*. Oxford: Oxbow Books. p 293–8.

Frisia S, Badertscher S, Borsato A, Susini J, Göktürk OM, Cheng H, Edwards RL, Kramers J, Tüysüz O, Fleitmann D. 2008. The use of stalagmite geochemistry to detect past volcanic eruptions and their environmental impacts. *PAGES News* 16(3):25–6.

LaMarche Jr VC, Hirschboeck KK. 1984. Frost rings in trees as records of major volcanic eruptions. *Nature* 307(5947):121–6.

Manning SW, Bronk Ramsey C, Kutschera W, Higham T, Kromer B, Steier P, Wild EM. 2006. Chronology for the Aegean Late Bronze Age 1700–1400 B.C. *Science* 312(5773):565–9.

Manning SW, Bronk Ramsey C, Kutschera W, Higham T, Kromer B, Steier P, Wild EM. 2009a. Dating Santorini/Thera eruption by radiocarbon: further discussion (AD 2006–2007). In: Manning SW, Bruce MJ, editors. *Tree-Rings, Kings, and Old World Archaeology and Environment*. Oxford: Oxbow Books. p 299–316.

Manning SW, Pulak C, Kromer B, Talamo S, Bronk Ramsey C, Dee M. 2009b. Absolute age of the Uluburun shipwreck: a key Late Bronze Age time-capsule for the East Mediterranean. In: Manning SW, Bruce MJ, editors. *Tree-Rings, Kings, and Old World Archaeology and Environment*. Oxford: Oxbow Books. p 163–87.

Manning SW, Kromer B, Bronk Ramsey C, Pearson CL, Talamo S, Trano N, Watkins JD. 2010. ^{14}C record and wiggle-match placement for the Anatolian (Gordion area) juniper tree-ring chronology ~1729 to 751 cal BC, and typical Aegean/Anatolian (growing season related) regional ^{14}C offset assessment. *Radiocarbon* 52(4):1571–97.

Manning SW, Kromer B. 2011. Radiocarbon dating archaeological samples in the Eastern Mediterranean, 1730 to 1480 BC: further exploring the atmospheric radiocarbon calibration record and the archaeological implications. *Archaeometry* 53(2):413–39.

Manning SW, Kromer B. 2012. Considerations of the scale of radiocarbon offsets in the east Mediterranean, and considering a case for the latest (most recent) likely date for the Santorini eruption. *Radiocarbon*, these proceedings.

Pasquier-Cardin A, Allard P, Ferreira T, Hatte C, Coutinho R, Fontugne M, Jaudon M. 1999. Magma-derived CO_2 emissions recorded in ^{14}C and ^{13}C content of plants growing in Furnas caldera, Azores. *Journal of Volcanology and Geothermal Research* 92(1–2): 195–207.

Reimer PJ, Baillie MGL, Bard E, Bayliss A, Beck JW, Blackwell PG, Bronk Ramsey C, Buck CE, Burr GS, Edwards RL, Friedrich M, Grootes PM, Guilderson TP, Hajdas I, Heaton TJ, Hogg AG, Hughen KA, Kaiser KF, Kromer B, McCormac FG, Manning SW, Reimer RW, Richards DA, Southon JR, Talamo S, Turney CSM, van der Plicht J, Weyhenmeyer CE. 2009. IntCal09 and Marine09 radiocarbon age calibration curves, 0–50,000 years cal BP. *Radiocarbon* 51(4): 1111–50.

Salzer MW, Hughes MK. 2007. Bristlecone pine tree rings and volcanic eruptions over the last 5000 yr. *Quaternary Research* 67(1):57–68.

Shaw I, editor. 2000. *The Oxford History of Ancient Egypt*. Oxford: Oxford University Press.

Steier P, Dellinger F, Kutschera W, Priller A, Rom W, Wild EM. 2004. Pushing the precision limit of ^{14}C AMS. *Radiocarbon* 46(1):5–16.

Steinhauser G, Sterba JH, Bichler M, Huber H. 2006. Neutron activation analysis of Mediterranean volcanic rocks – an analytical database for archaeological stratigraphy. *Applied Geochemistry* 21(8):1362–75.

Steinhauser G, Sterba JH, Oren E, Foster M, Bichler M. 2010. Provenancing of archaeological pumice finds from North Sinai. *Naturwissenschaften* 97(4):403–10.

Sterba JH, Polinger Foster K, Steinhauser G, Bichler M. 2009. New light on old pumice: the origins of Mediterranean volcanic material from ancient Egypt. *Journal of Archaeological Science* 36(8):1738–44.

Stuiver M, Polach HA. 1977. Discussion: reporting of ^{14}C data. *Radiocarbon* 19(3):355–63.

Tauber H. 1983. Possible depletion of ^{14}C in trees growing in calcareous soils. *Radiocarbon* 25(2):417–20.

Tronchère H, Salomon F, Callot Y, Goiran J-P, Schmitt L, Forstner-Müller I, Bietak M. 2008. Geoarchaeology of Avaris: first results. *Egypt and the Levant* 18:339–52.

Vinther BM, Clausen HB, Johnses SJ, Rasmussen SO, Andersen KK, Buchardt SL, Dahl-Jensen D, Seierstad IK, Siggard-Andersen M-L, Steffensen JP, Sevensson A. 2006. A synchronized dating of three Greenland ice cores throughout the Holocene. *Journal of Geophysical Research* 111: D13102.

Vogel JS, Southon JR, Nelson DE, Brown TA. 1984. Performance of catalytically condensed carbon for use in accelerator mass spectrometry. *Nuclear Instruments and Methods in Physics Research B* 5(2):289–93.

Warren P. 2009. The date of the Late Bronze Age eruption of Santorini. In: Warburton DA, editor. *Time's Up! Dating the Minoan Eruption of Santorini*. Athens: The Danish Institute at Athens. p 181–6.

Wiener MH. 2009. Cold fusion: the uneasy alliance of history and science. In: Manning SW, Bruce MJ, editors. *Tree-Rings, Kings, and Old World Archaeology and Environment*. Oxford: Oxbow Books. p 277–92.

Wild EM, Neugebauer-Maresch C, Einwögerer T, Stadler P, Steier P, Brock F. 2008. ^{14}C dating of the Upper Paleolithic site at Krems-Hundssteig in Lower Austria. *Radiocarbon* 50(1):1–10.

Wild EM, Gauß W, Forstenpointner G, Lindblom M, Smetana R, Steier P, Thanheiser U, Weninger F. 2010. ^{14}C dating of the Early to Late Bronze Age stratigraphic sequence of Aegina Kolonna, Greece. *Nuclear Instruments and Methods in Physics Research B* 268(7–8):1013–21.